ISIJ International, Vol. 48 (2008), No. 11, pp. 1524–1532

Materials Design for the Fabrication of Porous Glass using Phase Separation in Multi-component Borosilicate Glass

Masanori SUZUKI[1,2] and Toshihiro TANAKA[1]

1) Division of Materials and Manufacturing Science, Graduate School of Engineering, Osaka University, 2-1 Yamadaoka, Suita, Osaka 565-0871 Japan. 2) Research Fellow of the Japan Society for the Promotion of Science.

(*Received on May 30, 2008; accepted on July 30, 2008*)

Porous glass was fabricated using spinodal decomposition in multi-component oxide glass and leaching out one of the decomposed phases with acid solution. Multi-component borosilicate glass compositions were designed for the porous glass by partially replacing SiO_2 by B_2O_3 in silicate glass compositions where the occurrence of spinodal decomposition was confirmed. One of separated phases formed by the spinodal decomposition in the borosilicate glass was leached out with acid solution and then porous glass was obtained. The microstructure in porous glass was observed by field emission scanning electron microscopy, and the development of an interconnected porous structure was indicated. Prediction of the phase separation was attempted for multi-component borosilicate glass compositions investigated in this study by calculating the Gibbs energy of super-cooled liquid phase. It was revealed the calculated metastable liquid–liquid immiscibility boundaries in these borosilicate systems do not coincide with experimental results for the occurrence of phase separation. For the precise estimation of the miscibility gap in the multi-component oxide glasses containing B_2O_3, the temperature and composition dependence of Gibbs energy of liquid phase, including the super-cooled liquid state, should be optimized.

KEY WORDS: porous glass; spinodal decomposition; borosilicate glass; Gibbs energy; super-cooled liquid phase.

1. Introduction

Fabrication of porous glass using phase separation in glass has been performed for several oxide glasses.[1–4] In the preparation of porous glass, spinodal decomposition is important as a phenomenon of phase separation, because it forms three-dimensionally interconnected microstructures consisting of two different glass phases. The porous glass can be obtained by leaching out one of those phases with acid solution. Since its pore size can be easily changed at a nano-scale level, porous glass is expected to have widespread application; for instance, as filters to remove impurities from polluted water or air.

To create functional porous glass materials using waste slag discharged from metallurgical or waste melting processes, the authors have investigated the phase separation in multi-component oxide glass containing fundamental components in waste slag.[5,6] To generate phase separation in glass from waste slag, the composition ranges for metastable immiscibility and spinodal decomposition must be evaluated for multi-component slag systems. It is, however, difficult to predict the metastable immiscibility empirically for multi-component oxide systems such as waste slag. Therefore, it is necessary to perform a thermodynamic evaluation to determine the phase separation in multi-component oxide systems.

In previous studies,[5,6] the authors attempted to predict the composition ranges for metastable immiscibility and spinodal decomposition in the multi-component system SiO_2–CaO–MgO–Na_2O by calculating the composition dependence of the Gibbs energy in the super-cooled liquid phase. The occurrence of phase separation including spinodal decomposition was observed in heat-treated glasses, and the experimental results for phase separation corresponded to the calculated miscibility gap. One study[6] also revealed that the size of the microstructure formed by the metastable immiscibility depends on the initial glass compositions as well as the thermal conditions of heat-treatments.

The present study investigated materials design for creating porous glass using phase separation in multi-component oxide glass. SiO_2–CaO–Al_2O_3–Na_2O and SiO_2–CaO–MgO–Na_2O quaternary systems were selected for the production of porous glass, because it was found that composition ranges for phase separation in these quaternary systems can be evaluated by thermodynamic analyses. To remove one of separated phases with acid leaching, glass compositions in multi-component borosilicate systems were designed by partially substituting SiO_2 with B_2O_3 in the silicate glass compositions where the spinodal decomposition had been observed.

Since the morphology in porous glass depends on that in the two-phase decomposed glass before leaching, it is necessary to evaluate the possibility of metastable phase sepa-

ration for materials design relating to the fabrication of porous glass. In this paper, thermodynamic analyses were carried out to predict composition boundaries of the phase separation in multi-component oxide systems containing B_2O_3 using the Gibbs energy of the super-cooled liquid phase.

2. Estimation of the Metastable Miscibility Gap and Composition Range for Spinodal Decomposition[5)]

Liquid–liquid immiscibility can generally be evaluated from the Gibbs energy curve of the liquid phase. For instance, the miscibility gap in a binary system is determined from two points on the Gibbs energy curve with a common tangent. The composition range for spinodal decomposition, referred to as the "spinodal region" in the present work, is obtained from two inflexion points in the Gibbs energy curve.

In the present study, the possibility of phase separation including spinodal decomposition in glass was evaluated by calculating Gibbs energies and activities of SiO_2 in the metastable liquid phase, where glass in silicate systems is regarded as super-cooled metastable liquid phase. The Gibbs energies and activities of SiO_2 were calculated with the FactSage thermodynamic computing program with the F*A*C*T oxide databases for molten oxide systems.[7)] It has been found the use of these thermodynamic databases is valid for evaluating equilibrium phase relationships including those of liquid phases in several multi-component oxide systems.[8,9)]

It has been found that many binary silicate systems have metastable miscibility gaps at high concentrations of SiO_2.[10)] In our previous study,[5)] the Gibbs energy curves of the liquid phases were calculated for several binary silicate systems. The calculated results showed the Gibbs energies change almost linearly in SiO_2-rich composition ranges with the concentration of SiO_2. Therefore, it may be difficult to definitively determine the spinodal region from the inflexion points in the Gibbs energy curve for silicate systems.

Here the activity of SiO_2 in the super-cooled liquid phase is calculated using the concentration of SiO_2 to definitively determine the spinodal region. The composition range for spinodal decomposition is determined by differentiating the activity with respect to composition:

$$\frac{\partial a_B}{\partial X_B} = \frac{\exp(\mu_B / RT)}{RT} \cdot \frac{\partial \mu_B}{\partial X_B} = (1 - X_B) \frac{a_B}{RT} \cdot \frac{\partial^2 G^{Mix}}{\partial X_B^2} \quad \text{.....(1)}$$

where X_B is the mole fraction of component B and G^{Mix} represents the Gibbs energy for mixing in the liquid phase. μ_B and a_B denote the chemical potential and activity of component B respectively, and are expressed with respect to the pure liquid standard state as

$$\mu_B = RT \ln a_B = G^{Mix} + (1 - X_B) \frac{\partial G^{Mix}}{\partial X_B} \quad \text{.....(2)}$$

Equation (1) indicates the first differential of the activity with respect to the concentration of B is directly proportional to the second differential of the Gibbs energy with respect to composition. Since the second composition derivative of the Gibbs energy becomes zero at its inflexion points, the spinodal region is determined from extrema of the activity curve.

The above estimation procedure for the spinodal region can easily be extended to ternary or multi-component systems if one of the separated phases is a pure component. On the condition that pure component A constitutes one of the separated phases, the spinodal region in an A–B–C ternary system is evaluated by calculating the activity of component A across straight lines with a constant composition ratio of components B to C that correspond to tie-lines of the miscibility gap. For quaternary or multi-component systems, the spinodal region is evaluated similarly by calculating the activities of A in A–$B_{1-x}C_x$–D quasi-ternary systems (here x is 0 to 1).

In this study, metastable miscibility gaps in SiO_2–CaO–Al_2O_3–5mol%Na_2O and SiO_2–CaO–MgO–5mol%Na_2O quasi-ternary systems were calculated using the FactSage thermodynamic computing program. Spinodal regions in these systems were estimated by calculating the activities of SiO_2 in SiO_2–$(CaO)_{1-x}(Al_2O_3)_x$–Na_2O and SiO_2–$(CaO)_{1-x}(MgO)_x$–Na_2O (x is 0 to 1) quasi-ternary systems.

3. Experimental Procedure

3.1. Preparation of Two-phase Silicate Glass Materials

The occurrence of phase separation including spinodal decomposition was investigated experimentally to verify the calculated results for the metastable miscibility gaps. Silica, alumina, magnesia, sodium carbonate and calcium carbonate (all provided by Waco Corp. as special grade chemicals) were used to make glass materials.

First, $70SiO_2$–30mass%Na_2O glass was prepared as a mother glass to prevent the evaporation of Na_2O at high temperature. Silica and sodium carbonate were mixed in a mortar and melted in a Pt–10%Rh crucible in air for 3 h at 1 373 K. The mother glass was made by quenching the melt in water. X-ray diffraction analysis was carried out on the glass using a Rigaku RINT 2 500 V with CuKα radiation at 40 kV and 200 mA to examine whether a glass phase was obtained.

SiO_2–CaO–Al_2O_3–Na_2O and SiO_2–CaO–MgO–Na_2O glasses were prepared using silica, alumina, magnesia, calcium carbonate and the $70SiO_2$–30mass%Na_2O mother glass. These materials were mixed in a mortar and melted in Pt–10%Rh crucibles in air for 5 h at 1 873 K. Glass samples were obtained by quenching the melts in water and they were examined by X-ray diffraction analysis to determine whether they were glassy. The glasses were then heat-treated in air at a given temperature between 948 K and 993 K, and then cooled to room temperature. X-ray diffraction analysis was again performed on the heat-treated glasses to determine whether they retained their glass state. Microstructures in these glasses were observed by a HITACHI H800 transmission electron microscope using an excitation voltage of 200 kV and a camera length of 1.2 m. Preparation of the samples for electron microscopy was performed by an Ar-ion milling Gatan Model 691 with an ion-beam voltage of 4.0–4.5 kV.

3.2. Preparation of Two-phase Borosilicate Glass Materials

Two-phase multi-component borosilicate glasses were prepared to remove selectively one of the decomposed phases with acid solution and to produce porous glasses. The chemical compositions of the borosilicate glasses were designed by partially replacing the SiO_2 with B_2O_3 in silicate glass compositions in the spinodal regions of SiO_2–CaO–MgO–Na_2O and SiO_2–CaO–Al_2O_3–Na_2O systems.

B_2O_3–SiO_2–Na_2O glasses were made as a mother glass to prevent the evaporation of Na_2O and B_2O_3 at high temperature. Silica, boric acid and sodium carbonate were mixed in a mortar and melted in a Pt–10%Rh crucible in air for 1 h at 1 373 K. The mother glass was obtained by quenching the melt in water and used as a mother glass for the multi-component borosilicate glasses.

SiO_2–CaO–MgO–Na_2O–B_2O_3 and SiO_2–CaO–Al_2O_3–Na_2O–B_2O_3 glasses were produced by mixing calcium carbonate, magnesia, alumina and the B_2O_3–SiO_2–Na_2O mother glass, holding the samples in air for 5 h at 1 773 K, and then quenching the melts in water. After examining whether they were glassy with X-ray diffraction analysis, the glasses were annealed in air at a given temperature between 948 K and 993 K and then cooled to room temperature. X-ray diffraction analysis was again performed on the annealed glasses to determine whether they retained their glass state. Microstructures in these glasses were observed by transmission electron microscopy.

3.3. Fabrication of Porous Glass Materials using Phase Separation in Glass

Porous glass was produced from the two-phase glasses obtained from spinodal decomposition by leaching out one of decomposed phases with acid solution. 100 mg quantities of two-phase glass samples were used, the bulk sizes of which were adjusted to be less than 2 mm in diameter. The leaching process was performed by immersing the glasses in 100 ml of 1 M HCl solution at 353 K for 14 h in total, where acid solution was refreshed after immersing the glasses for 7 h. Microstructures on the surfaces of the glasses after leaching were observed using a Hitachi S-5200 field emission scanning electron microscope using an excitation voltage of 15 kV. Glass compositions dissolved in the acid solutions were analyzed with a Seiko SPS7800 inductively coupled plasma emission spectrometer.

4. Results and Discussion

4.1. Prediction of Phase Separation in the Glass SiO_2–CaO–Al_2O_3–Na_2O

Figure 1 shows the calculated activities of SiO_2 at 973 K in the super-cooled liquid phase of the SiO_2–CaO–Al_2O_3–Na_2O quaternary system. The activities of SiO_2 in the figure are calculated by varying the concentrations of SiO_2 while keeping the molar composition ratios of CaO to Al_2O_3 constant as 7/3. For any composition ratio of Na_2O to $7CaO \cdot 3Al_2O_3$, the activity of SiO_2 has a minimum for a high concentration of silica, and these results suggest metastable immiscibility where one of the separated phases can be regarded as pure SiO_2 metastable liquid phase.

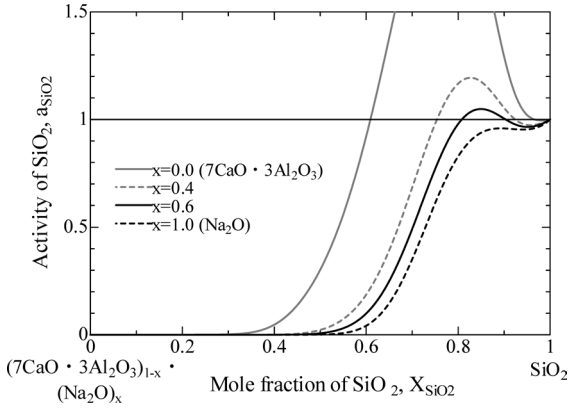

Fig. 1. Calculated activities of SiO_2 for the SiO_2–($7CaO \cdot 3Al_2O_3$)–Na_2O system at 973 K.

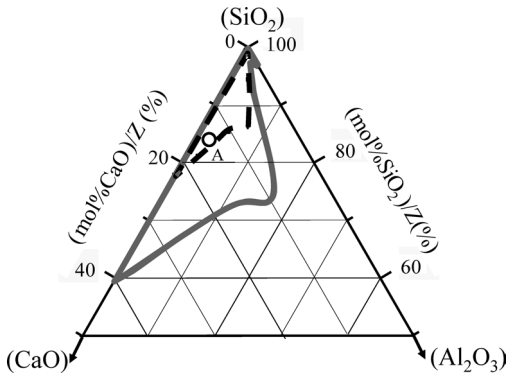

Fig. 2. Calculated composition ranges for phase separation and spinodal decomposition in the SiO_2–CaO–Al_2O_3–5mol%Na_2O system at 973 K (dashed line: composition range for spinodal decomposition; solid line: composition range for phase separation, Z=mol%(SiO_2+CaO+Al_2O_3)).

Figure 2 represents the calculated metastable miscibility gap and the spinodal region of the SiO_2–CaO–Al_2O_3–5mol%Na_2O system, where molar concentration of each component is divided by the sum of the molar concentrations of all components except Na_2O, *i.e.*:

$$(\mathrm{mol\%SiO_2})/Z(\%)=(\mathrm{mol\%SiO_2})/(\mathrm{mol\%SiO_2}+\mathrm{mol\%CaO}+\mathrm{mol\%Al_2O_3})\times 100$$

$$(\mathrm{mol\%CaO})/Z(\%)=(\mathrm{mol\%CaO})/(\mathrm{mol\%SiO_2}+\mathrm{mol\%CaO}+\mathrm{mol\%Al_2O_3})\times 100$$

$$(\mathrm{mol\%Al_2O_3})/Z(\%)=(\mathrm{mol\%Al_2O_3})/(\mathrm{mol\%SiO_2}+\mathrm{mol\%CaO}+\mathrm{mol\%Al_2O_3})\times 100 \quad \text{.....(3)}$$

The spinodal region in the system was determined by calculating the activities of SiO_2 in SiO_2–$(CaO)_{1-x}$-$(Al_2O_3)_x$–Na_2O (here x is 0 to 0.5) quasi-ternary systems, because the calculated activities of SiO_2 indicated a phase separation where one of the decomposed phases is regarded as pure SiO_2 metastable liquid phase, on the condition that molar ratios of CaO to Al_2O_3 were kept larger than unity. It is found from Fig. 2 that the width of the spinodal region increases as the molar composition ratio of CaO to Al_2O_3 increases.

The occurrence of phase separation by spinodal decomposition was investigated for glass A, which has a composi-

tion indicated by a white circle in Fig. 2. The chemical composition of glass A is shown in **Table 1**.

Table 2 shows the change in the appearance of glass A with holding time at 993 K. With increasing holding time, the glasses gradually turned adularescent. **Figure 3** shows X-ray diffraction patterns for glass A as quenched and after heat-treatment for 96 h at 993 K. Since crystalline peaks were not detected in the X-ray diffraction patterns for the annealed glass, the opaqueness was not attributed to the crystallization of glass.

Electron micrographs of glass A as quenched and after annealing are represented in **Fig. 4**. Development of morphology with interconnectivity was observed in the heat-treated glass. This interconnected microstructure indicates the occurrence of spinodal decomposition in the glass. Since no evidence of crystalline phases was detected in the electron diffraction pattern for each specimen in Fig. 4, it is revealed the annealed specimens were glassy in the microscopic observation area. Thus, the experimental result described above indicates spinodal decomposition occurs in the SiO_2–CaO–Al_2O_3–Na_2O glass according to the thermodynamic prediction of the metastable miscibility gap shown in Fig. 2.

Table 1. Composition of SiO_2–CaO–Al_2O_3–Na_2O glass sample.

	Composition [mol%]			
	SiO_2	CaO	Al_2O_3	Na_2O
A	80.8	11.7	2.5	5.0

Table 2. Change in appearance of glass A during heat treatment.

	Heating time [h] (Temperature: 993 K)		
	24	48	96
A	transparent →	adularescent →	adularescent

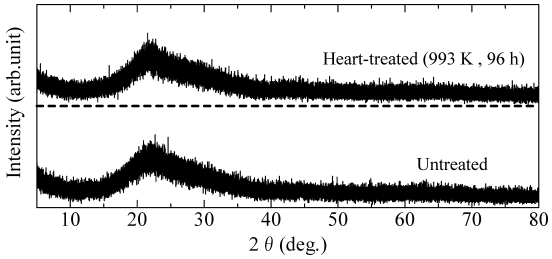

Fig. 3. XRD patterns of glass A heat-treated for 96 h at 993 K.

4.2. Prediction of Phase Separation in the Glass SiO_2–CaO–MgO–Na_2O[5,6]

The calculated results of the metastable miscibility gap and the spinodal region of the SiO_2–CaO–MgO–5mol%Na_2O system at 948 K are shown in **Fig. 5**, where molar concentration of each component is divided by the sum of the molar concentrations of all components except Na_2O. The spinodal region in the system was obtained by calculating the activities of SiO_2 in SiO_2–$(CaO)_{1-x}(MgO)_x$–Na_2O (here x is 0 to 1) quasi-ternary systems, because the calculated results of activities of SiO_2 in the super-cooled liquid phase indicated one of the separated phases in the metastable immiscibility is regarded as pure SiO_2 metastable liquid phase.[5] Figure 5 shows that spinodal decomposition occurs in the composition range indicated by the dotted line and that binodal decomposition occurs in the range indicated by the solid line.

The occurrence of phase separation was investigated for the glasses B–E, having compositions indicated by square marks in Fig. 5, by producing two-phase glasses and observing microstructures in those glasses. The chemical compositions of glasses B–E are shown in **Table 3**.

Figure 6 shows electron micrographs of glasses B–E heated for 192 h at 948 K, and indicates the microstructure formed by phase separation. In glass B, interconnected microstructure was observed, and this structure corresponds to

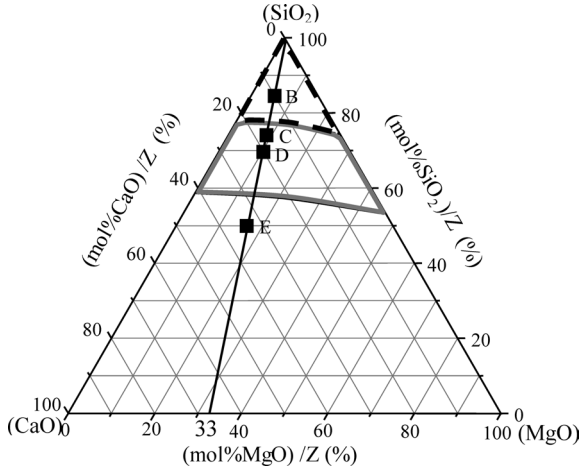

Fig. 5. Calculated composition ranges for phase separation in the SiO_2–CaO–MgO–5mol%Na_2O system at 948 K (dashed line: composition range for spinodal decomposition; solid line: composition range for binodal decomposition, Z= mol%(SiO_2+CaO+MgO)).

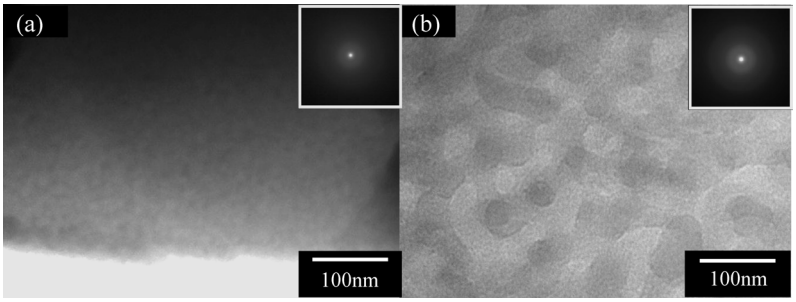

Fig. 4. Electron micrographs of glass A; (a) untreated, (b) heat-treated for 96 h at 993 K.

spinodal decomposition. The cross-section of the interconnected microstructure is estimated to be 80 to 100 nm in diameter. In glasses C and D, particle structures corresponding to phase separation by binodal decomposition were observed. As the composition of glass E was outside the miscibility gap, no specific microstructure was observed after heat-treatment for 192 h. Since the electron diffraction pattern for each specimen in Fig. 6 showed no evidence of crystalline phases, it is suggested the annealed specimens were glassy in the microscopic observation area.

The above experimental results indicate the microstructures observed in the heat-treated glasses can be attributed to the phase separation in glass and that phase separation including spinodal decomposition occurs in the SiO_2–CaO–MgO–Na_2O glasses in accordance with the thermodynamic prediction of the metastable miscibility gap shown in Fig. 5.

4.3. Fabrication of Porous Glass Materials Using Spinodal Decomposition in Glass

In the present study, creation of porous glass was attempted using two-phase glasses obtained from spinodal decomposition by removing one of decomposed phases with acid solutions.

Frst, the leaching process was performed for glass B in the SiO_2–CaO–MgO–Na_2O system because the occurrence of spinodal decomposition was observed in the annealed glass B. **Table 4** presents the proportion of weight composition in glass B dissolved in the acid solution. The table indicates the concentrations of SiO_2, CaO, MgO and Na_2O dissolved in the acid solution are quite low. Since the phases decomposed by spinodal decomposition in glass B contain high concentrations of SiO_2, it may be difficult to remove one of the phases selectively by acid leaching.

Previous experimental studies[1–4] have revealed that in the spinodal decomposition in glasses containing B_2O_3, one of the separated phases includes much B_2O_3 and can be leached out with acid solutions. In this study, multi-component borosilicate glass compositions A-2 and B-2 were designed by partially substituting SiO_2 with B_2O_3 in glasses A and B, for which compositions were included in the spinodal regions of SiO_2–CaO–Al_2O_3–Na_2O and SiO_2–CaO–MgO–Na_2O systems. The chemical compositions of the borosilicate glasses are presented in **Table 5**. Glass compositions A-2 and B-2 were determined by replacing 30 mol% of SiO_2 in glasses A and B with $BO_{1.5}$, while keeping the sum of the molar concentrations of all components including B_2O_3 as 100 mol%. These compositions have been selected to let the mass composition ratios of B_2O_3 : SiO_2 : Na_2O exist in the immiscibility region of the B_2O_3–SiO_2–Na_2O system found in many previous experimental studies[1] as shown in **Fig. 7**. Thus, the composition ratios of B_2O_3 : SiO_2 : Na_2O in glasses A-2 and B-2 are equal to each other.

Table 3. Composition of SiO_2–CaO–MgO–Na_2O glass samples.

	Composition [mol%]			
	SiO_2	CaO	MgO	Na_2O
B	80.8	9.5	4.7	5.0
C	71.3	15.8	7.9	5.0
D	66.5	19.0	9.5	5.0
E	47.5	31.7	15.8	5.0

Table 4. Loss of components in two-phase glass B by acid leaching.

	Weight of dissolved components / Weight of components in initial glass (%)			
	SiO_2	CaO	MgO	Na_2O
B	0.19	2.95	0.26	0.025

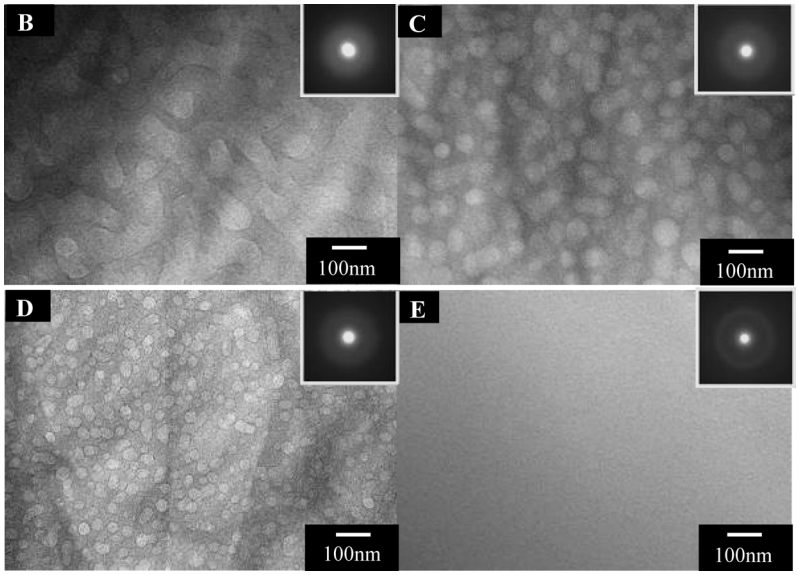

Fig. 6. Electron micrographs for glasses B, C, D and E heat-treated for 192 h at 948 K.

Table 5. Composition of borosilicate glass samples.

	Composition [mol%]					
	SiO_2	CaO	Al_2O_3	MgO	Na_2O	B_2O_3
A-2	59.7	13.8	2.9	—	5.9	17.7
B-2	59.7	11.2	—	5.6	5.9	17.7

Tables 6 and **7** show the change in appearance of glasses A-2 and B-2 during the heat-treatment and leaching. With an increasing holding time in the heat-treatment, glass A-2 gradually turned a transparent bluish color and then opaque. Glass B-2 was already opaque before heat-treatment and retained its appearance during annealing. After leaching, the appearances of both the glasses did not change. **Figures 8** and **9** present X-ray diffraction patterns for glasses A-2 and B-2 after heat-treatment and leaching. Since crystalline peaks were not detected in the X-ray diffraction patterns, the opaqueness was not attributed to the crystallization of glass.

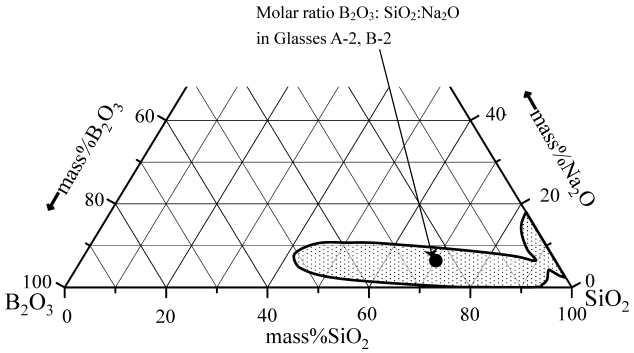

Fig. 7. Miscibility gap in B_2O_3–SiO_2–Na_2O system at 973 K reported by Haller *et al.*,[1] showing materials design for the phase separation in multi-component borosilicate systems.

The microstructures in glass A-2 after heat-treatment and leaching are shown in **Fig. 10**. Morphology with interconnectivity was observed after heat-treatment, and the microstructure indicates the occurrence of spinodal decomposition in glass. As shown in Fig. 10(b), the interconnected porous structure was present in glass A-2 after leaching and corresponded to the microstructure in the annealed glass in Fig. 10(a). The cross-section of the remaining phase in the porous glass was estimated to be 500 nm in diameter. Thus, porous glass material was obtained from spinodal decomposition in the SiO_2–CaO–Al_2O_3–Na_2O–B_2O_3 multi-component glass, and one of the decomposed phases was leached out with acid solution.

Figure 11 shows the microstructures in the SiO_2–CaO–MgO–Na_2O–B_2O_3 multi-component glass B-2 after heat-treatment and leaching. Particle microstructure indicating binodal decomposition was observed after heat-treatment. This microstructure is different from the interconnected structure present in the annealed glass A-2. The three-dimensional particle structure was obtained in glass B-2 after

Table 6. Change in appearance of glass A-2 during heat treatment and acid leaching.

	Holding time [h] (Temperature: 993 K)			Acid
	24	48	96	leaching
A-2	bluish transparent →	opalescent →	opalescent	

Table 7. Change in appearance of glass B-2 during heat treatment and acid leaching.

	Holding time [h] (Temperature: 948 K)			Acid
	24	48	96	leaching
B-2	opalescent →	opalescent →	opalescent	

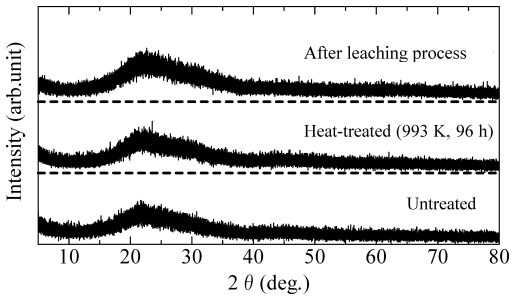

Fig. 8. XRD patterns for glass sample A-2 after heat-treatment and acid leaching.

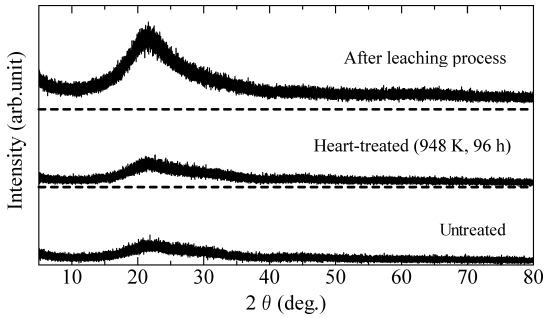

Fig. 9. XRD patterns for glass sample B-2 after heat-treatment and acid leaching.

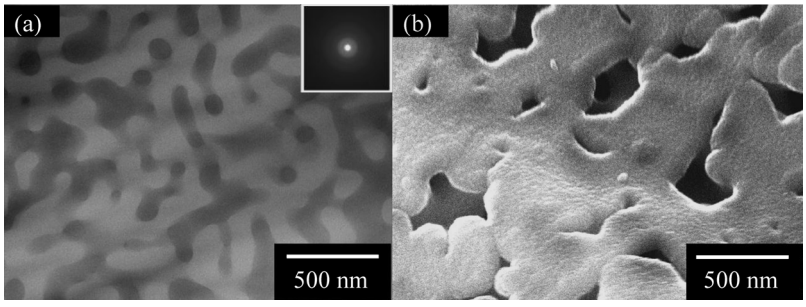

Fig. 10. Scanning electron micrographs of the surfaces of glass A-2: (a) after heat- treatment, (b) after leaching.

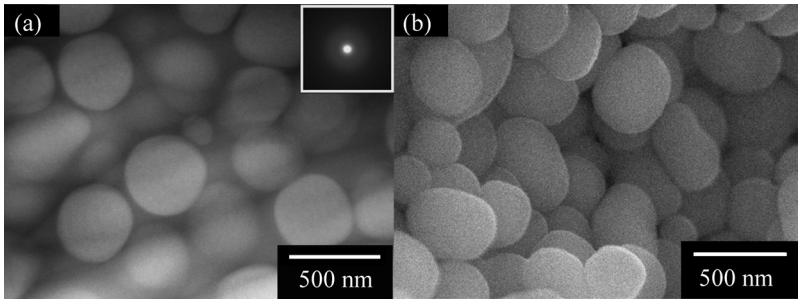

Fig. 11. Scanning electron micrographs of the surfaces of glass B-2: (a) after heat- treatment, (b) after leaching.

Table 8. Loss of components in two-phase glasses A-2 and B-2 by acid leaching.

	Weight of dissolved components / Weight of components in initial glass (%)					
	SiO_2	CaO	Al_2O_3	MgO	Na_2O	B_2O_3
A-2	22.4	100.0	28.1	—	1.0	80.0
B-2	28.1	100.0	—	100.0	3.2	74.2

Table 9. Compositions of dissolved phase and remaining phase in glasses A-2 and B-2.

		Compositions [mass%]					
		SiO_2	CaO	Al_2O_3	MgO	Na_2O	B_2O_3
A-2	Dissolved phase	32.8	33.4	3.8	—	0.1	29.9
	Remaining phase	81.8	0.0	6.9	—	5.9	5.4
B-2	Dissolved phase	38.8	25.8	—	10.2	0.2	25.0
	Remaining phase	87.5	0.0	—	0.0	4.8	7.7

Table 10. Morphology of microstructures formed by phase separation in multi-component silicate and borosilicate glass samples.

	Silicate Glasses		Borosilicate Glasses	
	A	B	A-2	B-2
Morphology of microstructure	Interconnected structure	Interconnected structure	Interconnected structure	Particle structure

leaching, as shown in Fig. 11(b). Since this particle structure corresponds to the microstructure in the two-phase glass B-2, the matrix glass phase is considered to have been removed with acid solution.

Table 8 represents the ratios of compositions in the two-phase glasses A-2 and B-2 dissolved in acid solutions to those in the initial glass phases. The chemical compositions of dissolved phases and remaining phases in the glasses A-2 and B-2 were also analyzed and summarized in **Table 9**. Tables 8 and 9 indicate that much CaO, MgO and B_2O_3 in these glasses were dissolved in acid solutions, and that remaining phases include a high concentration of SiO_2.

4.4. Prediction of Phase Separation in Multi-component Oxide Glasses Containing B_2O_3 to Design Glass Compositions for the Porous Glass Materials

Table 10 summarizes the morphology of microstructures formed by phase separation in multi-component silicate glasses A and B, and borosilicate glasses A-2 and B-2, the compositions of which were selected by partially replacing SiO_2 with B_2O_3 in glasses A and B. Although interconnected microstructures are obtained in glasses A and B, the two-phase morphology in glass A-2 is different from that in glass B-2; *i.e.*, an interconnected structure forms in glass A-2 and particle structure is present in glass B-2. When porous glass is obtained by leaching one of the decomposed phases with acid solutions, the morphology in the porous glass is dependent on the morphology in the two-phase glass before leaching. Therefore, to design glass compositions for the fabrication of porous glass using phase separation, the possibility of the metastable immiscibility should be predicted for multi-component oxide systems containing B_2O_3.

In this study, the prediction of the phase separation in borosilicate glasses A-2 and B-2 was attempted by calculating the composition dependence of the Gibbs energy of the super-cooled liquid phase because the calculated metastable miscibility gaps corresponded to the experimental results for the occurrence of phase separation in multi-component silicate glasses.[5,6] The calculated results are presented in **Table 11**. Although the occurrence of phase separation was confirmed experimentally in glass A-2, the calculated result suggested phase separation would not occur for the glass composition. Thus, the calculated results of the possibility of metastable immiscibility do not correspond to the experimental results in multi-component oxide glasses containing B_2O_3. To precisely evaluate the metastable miscibility gap, the temperature and composition dependence of the Gibbs energy function of the liquid phase should be optimized in multi-component borosilicate systems.

It should be noted that, in the thermodynamic oxide data-

Table 11. Calculated results of the possibility of phase separation in multi-component borosilicate glasses (holding temperature: 973 K).

		Composition [mass%]					
		SiO_2	CaO	Al_2O_3	MgO	Na_2O	B_2O_3
A-2	Initial glass	57.3	12.4	4.8	—	5.8	19.7
	Phase separation does not occur						
B-2	Initial glass	59.4	10.4	—	3.8	6.0	20.4
	Separated phase 1	27.8	12.5	—	12.1	7.6	40.0
	Separated phase 2	72.5	9.5	—	0.4	5.3	12.3

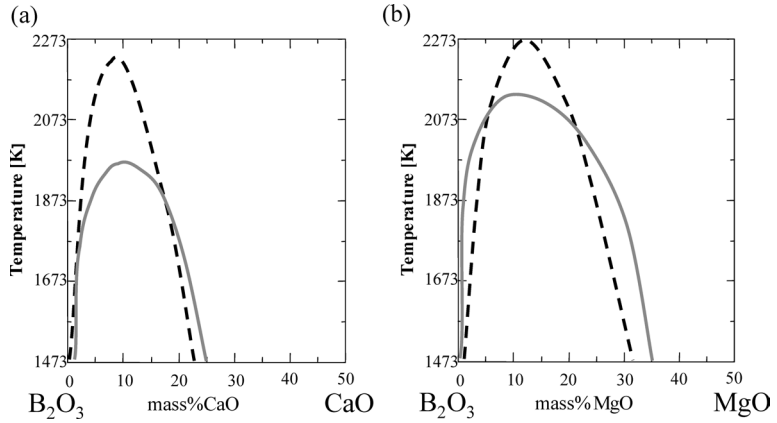

Fig. 12. Calculated liquid–liquid immiscibility boundaries in (a) B_2O_3–CaO and (b) B_2O_3–MgO systems (dashed line: calculated; solid line: experimental[11]).

bases used in this study,[7] the Gibbs energy function of liquid phase in multi-component borosilicate systems is expressed by the summation of those functions in binary borate systems, ternary borate systems and multi-component silicate systems except for B_2O_3, as shown in the following equation.

$$G^{\mathrm{Mix}}\left(\begin{matrix}\text{Multi-component}\\ \text{borosilicate systems}\end{matrix}\right)=\sum G^{\mathrm{Mix}}\left(\begin{matrix}\text{Binary systems}\\ \text{including } B_2O_3\end{matrix}\right)+\sum G^{\mathrm{Mix}}\left(\begin{matrix}\text{Ternary systems}\\ \text{including } B_2O_3\end{matrix}\right)+\sum G^{\mathrm{Mix}}\left(\begin{matrix}\text{Multi-component silicate}\\ \text{systems except } B_2O_3\end{matrix}\right) \quad \text{.....(4)}$$

Our previous studies revealed the metastable miscibility gaps calculated by the Gibbs energy of the liquid phase corresponds to the experimental results for phase separation in multi-component silicate systems except for B_2O_3.[5,6] Therefore, thermodynamic analyses must be performed to examine whether the phase relationships in fundamental binary and ternary borate systems are estimated precisely using the current Gibbs energy functions, for the further evaluation of phase relations in multi-component borosilicate systems.

Figure 12 shows the calculated stable miscibility gaps in B_2O_3–CaO and B_2O_3–MgO binary systems, as compared with experimental results on the liquid–liquid phase separation.[11] In these binary borate systems, it is suggested the calculated immiscibility boundaries correspond to the previous experimental results.

The metastable miscibility gaps were calculated in B_2O_3–SiO_2 and B_2O_3–Na_2O systems using the Gibbs energy of super-cooled liquid phase and are presented in **Fig. 13**. The calculated immiscibility boundary in the B_2O_3–SiO_2 system coincides with experimental values for critical temperatures for phase separation.[12] Although the occurrence of phase separation is reported in the B_2O_3–Na_2O system for a high concentration of B_2O_3,[13] the calculated result using the Gibbs energy of super-cooled liquid phase does not suggest the possibility of phase separation in this composition range.

The estimation of the metastable immiscibility boundary was carried out in the ternary system B_2O_3–SiO_2–Na_2O, and the calculated result is shown in **Fig. 14**. The figure indicates there is obvious disagreement between the calculated and experimental results[1] for the immiscibility boundaries.

The above calculated results indicate that if previous experimental results on phase separation are correct, the temperature or composition dependence of the Gibbs energies of the liquid phase in the binary system B_2O_3–Na_2O and ternary system B_2O_3–SiO_2–Na_2O should be modified for the evaluation of metastable immiscibility in multi-component borosilicate systems. The Gibbs energy coefficients in B_2O_3–SiO_2 system might also be optimized because the calculated miscibility gap in the B_2O_3–SiO_2 system is not in the silica-rich composition range, in spite of experimental results for the occurrence of phase separation at a high concentration of SiO_2 in the B_2O_3–SiO_2–Na_2O system.

5. Conclusions

Materials design was attempted for the fabrication of porous glass using spinodal decomposition in multi-component oxide glass. In the experimental study, multi-com-

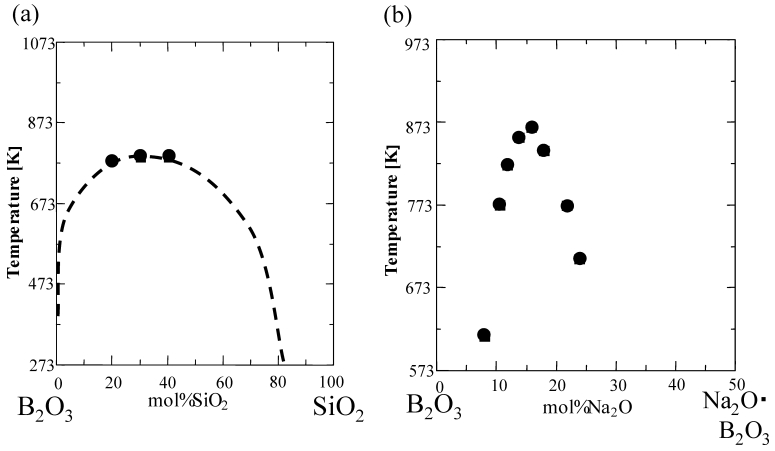

Fig. 13. Calculated metastable immiscibility boundaries in (a) B_2O_3–SiO_2 and (b) B_2O_3–Na_2O systems (dashed line: calculated; black circles: experimental[12,13]).

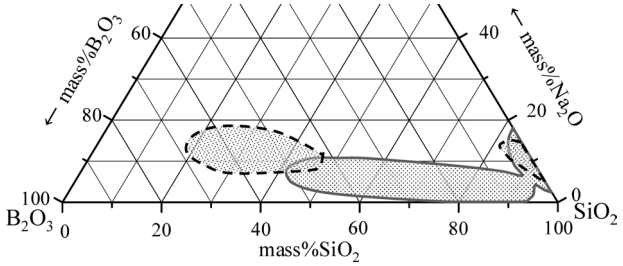

Fig. 14. Comparison between calculated and experimental results of the metastable miscibility gap in B_2O_3–SiO_2–Na_2O system at 973 K (dashed line: calculated; solid line: experimental[1]).

ponent borosilicate glasses were produced by partially replacing SiO_2 with B_2O_3 in the SiO_2–CaO-Al_2O_3–Na_2O and SiO_2–CaO–MgO–Na_2O glass compositions where the occurrence of spinodal decomposition was confirmed. One of phases separated by spinodal decomposition in these borosilicate glasses were removed by acid leaching and a porous glass having three-dimensional interconnected structure was obtained from SiO_2–CaO–Al_2O_3–Na_2O–B_2O_3 multi-component glass. On the other hand, a three-dimensional particle structure formed in SiO_2–CaO–MgO–Na_2O–B_2O_3 glass after the leaching. This particle structure is due to the binodal decomposition in the multi-component glass.

Thermodynamic analyses were carried out to predict the composition range for phase separation in multi-component borosilicate glasses, using the composition dependence of the Gibbs energy of the super-cooled liquid phase. Although the occurrence of phase separation was confirmed experimentally in the borosilicate glasses described above, the calculated results for the possibility of metastable immiscibility do not coincide with the experimental results. To precisely estimate the metastable miscibility gap in the multi-component oxide glasses containing B_2O_3, the temperature and composition dependence of Gibbs energy of liquid phase, including the super-cooled liquid state, should be modified.

Acknowledgements

This study was supported by Priority Assistance for the Formation of Worldwide Renowned Centers of Research—The Global COE Program (Project: Center of Excellence for Advanced Structural and Functional Materials Design) from the Ministry of Education, Culture, Sports, Science and Technology (MEXT), Japan.

Observation of the microstructures in the samples by electron microscopy was supported by Professor Hirotaro Mori and technical official Eiji Taguchi (Research Center for Ultra-high Voltage Electron Microscopy, Osaka University) and carried out in a facility at the Research Center for Ultra-high Voltage Electron microscopy, Osaka University. We thank them most warmly for their assistance in this study.

REFERENCES

1) W. Haller, D. H. Blackburn, F. E. Wagstaff and R. J. Charles: *J. Am. Ceram. Soc.*, **53** (1970), 34.
2) T. H. Elmer, M. E. Nordberg, G. B. Carrier and E. J. Korda: *J. Am. Ceram. Soc.*, **53** (1970), 171.
3) T. Nakashima and Y. Kuroki: *Nippon Kagaku Kaishi*, (1981), 1231.
4) T. Kokobu and M. Yamane: *J. Mater. Sci.*, **20** (1985), 4309.
5) M. Suzuki and T. Tanaka: *ISIJ Int.*, **46** (2006), 1391.
6) M. Suzuki and T. Tanaka: *ISIJ Int.*, **48** (2008), 405.
7) C. W. Bale, A. D. Pelton, W. T. Thompson and G. Eriksson: FactSage, Ecole Poly-technique, Montreal, (2001), http://www.crct.polymtl.ca. (Accessed on 3rd, April, 2008).
8) S. Degterov and A. D. Pelton: *Metall. Mater. Trans B*, **28B** (1997), 235.
9) Y. B. Kang, I. H. Jung, S. A. Decterov, A. D. Pelton and H. G. Lee: *ISIJ Int.*, **44** (2004), 975.
10) W. Haller, D. H. Blackburn and J. H. Simmons: *J. Am. Ceram. Soc.*, **57** (1974), 120.
11) V. B. M. Hageman and H. A. J. Oonk: *Phys. Chem. Glasses*, **28** (1987), 183.
12) R. J. Charles and F. E. Wagstaff: *J. Am. Ceram. Soc.*, **51** (1968), 16.
13) R. R. Shaw and D. R. Uhlmann: *J. Am. Ceram. Soc.*, **51** (1968), 377.